On the nature of precursor flows upstream of advancing dipolarization fronts

X.-Z. Zhou,[1] V. Angelopoulos,[1] V. A. Sergeev,[2] and A. Runov[1]

Received 30 September 2010; revised 29 December 2010; accepted 11 January 2011; published 18 March 2011.

[1] Earthward propagating dipolarization fronts, interpreted as thin, vertical current sheets that separate plasmas of different origins in the Earth's magnetotail, are embedded within flow bursts, often near the leading edge of bursty bulk flows. Observations have also shown that bursty bulk flow onset typically precedes dipolarization front arrival by ~1 min. Ion distribution functions reveal that earthward flows in advance of front arrival are often caused by the appearance of a new ion population atop a preexisting plasma sheet component. Particle simulations suggest that this second population, which contributes most to the plasma velocity, is composed of ions that have been reflected at and accelerated by the approaching front. We propose that in the presence of a finite upstream B_z field, the reflected ions would be confined in a region with a size comparable to the ion thermal gyroradius over the upstream B_z. THEMIS observations confirm that the measured time difference δt between the appearance of earthward plasma flows and the dipolarization front arrival is consistent with the predicted size of the ion accessibility region.

Citation: Zhou, X.-Z., V. Angelopoulos, V. A. Sergeev, and A. Runov (2011), On the nature of precursor flows upstream of advancing dipolarization fronts, *J. Geophys. Res.*, *116*, A03222, doi:10.1029/2010JA016165.

1. Introduction

[2] Bursty bulk flows (BBFs), containing transient, high-speed plasma flows responsible for a significant portion of flux transport in the Earth's magnetotail [*Angelopoulos et al.*, 1992, 1994], have been often observed to be associated with strong (~1–10 nT), abrupt (~0.5–5 s) enhancements of the magnetic field B_z component. These transient enhancements, usually preceded by a minor B_z decrease and followed by a gradual B_z decrease, have been termed dipolarization fronts (DFs) [*Nakamura et al.*, 2002; *Sergeev et al.*, 2009; *Runov et al.*, 2009, 2011a].

[3] Dipolarization fronts observed in the magnetotail plasma sheet are usually interpreted as signatures of either BBF-type flux ropes [*Slavin et al.*, 2003; *Zong et al.*, 2004], or nightside flux transfer events [*Sergeev et al.*, 1992; *Semenov et al.*, 2005]. Recent observations and kinetic simulations have suggested that most dipolarization front signatures, including the steep front, the B_z dip preceding the front, and the gradual B_z decrease following it, are likely to be remote signatures of transient reconnection [*Sitnov et al.*, 2009; *Runov et al.*, 2011a].

[4] Unlike the classical signatures of magnetic dipolarization, which have been associated with the reduction of cross-tail current and the formation of substorm current wedge [*McPherron et al.*, 1973; *Lui et al.*, 1988], dipolarization fronts are accompanied by significant enhancements of current density in the dawn-dusk direction within the plasma sheet [*Runov et al.*, 2011a, 2011b; *Zhang et al.*, 2011]. After their generation in the midtail region, the fronts have been observed to coherently propagate earthward near the leading edge of plasma flows, as vertical thin current sheets separating freshly heated, usually underpopulated plasma from the ambient colder and denser plasma sheet population [*Runov et al.*, 2009; *Sergeev et al.*, 2009].

[5] The onset of earthward plasma bulk flows does not coincide with arrival of the dipolarization front. In fact, observations have shown that enhancement of earthward plasma velocity v_x, usually accompanied by enhancements of plasma density and plasma pressure, typically appears ~1 min before the dipolarization front [*Ohtani et al.*, 2004; *Sergeev et al.*, 2009, 2011; *Dubyagin et al.*, 2010].

[6] It has been suggested that flows preceding dipolarization fronts are consistent with the "bubble" theory [*Pontius and Wolf*, 1990; *Chen and Wolf*, 1993], in which ambient plasma tubes are displaced sideways by a penetrating "bubble" [*Sergeev et al.*, 1996]. As shown in a case study of the interaction between the curvature force and the ambient plasma pressure [*Li et al.*, 2011], the MHD description can be an effective way to describe propagation of dipolarization fronts and the establishment of a flow field surrounding them. After repeated damped oscillations of BBFs within the plasma sheet, the force imbalance has been shown to relax, again due to the change of pressure gradients [*Panov et al.*, 2010]. Thus, earthward precursor flows can be explained as the result of plasma compression.

[1] Institute of Geophysics and Planetary Physics, University of California, Los Angeles, California, USA.
[2] Institute of Physics, St. Petersburg State University, St. Petersburg, Russia.

0148-0227/11/2010JA016165

[7] However, a kinetic picture may be equivalent, or even more appropriate on some occasions. Examination of the observed ion distributions within the 29 March 2009 substorm/dipolarization front event [*Sergeev et al.*, 2011] suggested different patterns of the earthward flows before and after the front arrival. Although the ion population after the front has a single component moving earthward, the ions ahead of the front are actually the superposition of a gradually emerging earthward streaming component and the preexisting plasma sheet population [*Zhou et al.*, 2010] (hereinafter referred to as Zhou10). These observational signatures were well reproduced by test particle simulations (see Zhou10), suggesting that the superposed earthward streaming ion population is composed of ions that have been reflected and accelerated by the approaching front.

[8] In this paper, we attempt to quantify the relationship between the durations of precursor flows in advance of dipolarization fronts and ambient parameters, and to find evidence on how important and how common the particle acceleration picture is. In section 2, after briefly describing our simulation technique, we make use of a more realistic model of the equilibrium current sheet (with a finite magnetic field in the sheet-normal direction) as the initial condition, to discuss the ion behavior upstream of the front. Predictions can thus be made concerning factors that may affect the length of the time interval (hereinafter referred to as δt) between the appearances of the earthward flow and the dipolarization front. In section 3, statistical studies based on THEMIS' comprehensive coverage of the near-Earth magnetotail with its inner 3 probes, P3, P4 and P5 [*Sibeck and Angelopoulos*, 2008, Figure 10], are also conducted to verify these predictions.

2. Simulations

[9] Two steps are required to simulate the observed ion distributions ahead of earthward propagating dipolarization fronts. The first is to determine the initial condition, namely, the plasma populations and magnetic profiles of the tail current sheet in the equilibrium state, before appearance of the earthward flow and front arrival. *Zhou et al.* [2009b] have suggested that magnetic profiles as well as particle distributions everywhere within the equilibrium current sheet could be self-consistently determined on the basis of single-point observations, by selecting an appropriate kinetic model (with several free parameters) [e.g., *Harris*, 1962; *Schindler and Birn*, 2002; *Yoon and Lui*, 2004; *Sitnov et al.*, 2006] and fitting the observed particle distributions with the modeled ones.

[10] With the initial condition determined, test particle simulations can then be carried out under prescribed electric and magnetic fields, as the second step, to simulate the evolution of ion distributions [*Zhou et al.*, 2009a]. Here the association between the ion distributions in the initial equilibrium and those at later times is provided by Liouville's theorem [*Schwartz et al.*, 1998; *Wanliss et al.*, 2002]. In other words, the ion distributions $f(\mathbf{r}, \mathbf{v}, t)$ at time t can be obtained by tracing ion trajectories backward in time to identify their initial locations $\mathbf{r}_0$ and velocities $\mathbf{v}_0$ within the modeled equilibrium at t_0 and equating $f(\mathbf{r}, \mathbf{v}, t)$ with the corresponding $f(\mathbf{r}_0, \mathbf{v}_0, t_0)$ values.

[11] In previous work [*Zhou et al.*, 2010], a case-oriented one-dimensional current sheet model, which is a modification of the traditional *Harris* [1962] model, was selected as the initial equilibrium. The magnetic field in the equilibrium solution is always in the x direction (with no B_z field), which is assumed to remain the same as the dipolarization front approaches. In addition, a B_z field, described by

$$B_z(x,t) = \frac{B_f}{2}\left\{1 - \tanh\left[\frac{x - x_{f0} - v_f(t - t_0)}{L_f}\right]\right\}, \quad (1)$$

was added to the initial equilibrium to represent the earthward propagation of a hyperbolic tangent front at a speed of v_f. Here B_f is the B_z enhancement associated with the dipolarization front; L_f is the characteristic half thickness of the front; and x_{f0} is the location of the dipolarization front at $t = t_0$. Also superposed in the model is a dawn-dusk electric field

$$E_y(x,t) = v_f B_z, \quad (2)$$

built up in accordance with Faraday's law to model the electric field associated with the earthward propagation of the front.

[12] The values of the parameters, used by Zhou10, were determined from the observations, in order to provide a reasonable simplification of the field geometry during the 29 March 2009 substorm event. The ion trajectory calculations and subsequent Liouville mappings revealed upstream distributions similar to those observed by THEMIS [*Sergeev et al.*, 2011]: the gradual emergence of an earthward streaming ion population superimposed on the preexisting duskward streaming ambient ions that carry the cross-tail current. This new, earthward streaming ion population was accelerated and reflected by the earthward propagating front.

[13] A salient feature of the simulations of Zhou10, however, did not fully agree with THEMIS observations: the earthward streaming ion population appeared nearly 2 min ahead of the front in the simulations, but only ~1 min in the observations. we investigated the hypothesis that this discrepancy comes from an unrealistic, infinite y scale of the modeled front of Zhou10. We found that the introduction of a localized front in the simulations improves the results only slightly.

[14] In this section, we propose a different explanation for this timing discrepancy. We postulate that the discrepancy arises from the absence of a background B_z field in our oversimplified equilibrium current sheet model. We introduce a more realistic model with a finite B_z as the initial condition to replace the 1-D model employed by Zhou10, and demonstrate a good agreement with the observed timing of flow onset. By varying systematically the model parameters we then verify the expectation, based on first principles, that the size of the ion accessibility region upstream of the front is governed, in our model, by the front speed, the upstream ion thermal speed and the upstream B_z.

[15] By making these attempts, we intend to better understand particle acceleration processes associated with dipolarization fronts, and therefore to provide clues on the global structure and propagation of the front through the plasma sheet.

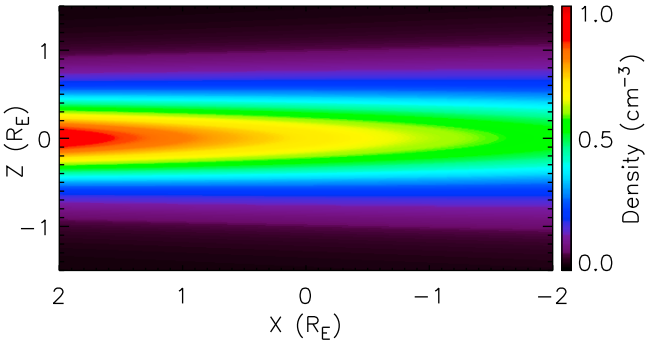

Figure 1. Plasma density distributions within the initial equilibrium, with the isodensity lines also delineating magnetic field lines.

[16] The revised equilibrium current sheet model used herein can be found in work by *Pritchett and Büchner* [1995]. It is an analytical solution of the two-dimensional Vlasov-Maxwell equations [*Schindler*, 1972; *Lembége and Pellat*, 1982; *Manankova*, 2003]. Its key element is a generalization of the traditional *Harris* [1962] model: assuming that particle distributions are functions of two invariants of motion (the particle energy W and the canonical momentum P_y), the Vlasov equation is automatically satisfied, and the substitution of the particle distribution moments in the Maxwell equations suggests solutions of the equilibrium current sheet. In the presence of both B_x and B_z, the substitution results in the following equation:

$$\nabla^2 A_y = \left(d^2/dz^2 + d^2/dx^2\right)A_y = -\mu_0 J\left(A_y\right), \tag{3}$$

where $J(A_y)$, a function of magnetic vector potential A_y, is the electric current in the y direction. This equation yields a self-consistent solution of the two-dimensional equilibrium current sheet, with the magnetic field obtained from the vector potential given by

$$A_y(x,z) = B_0 L \ln\{\cosh[F(x)(z/L)]/F(x)\}, \tag{4}$$

where $F(x)$ is a slowly varying but otherwise arbitrary function, and L is the nominal half thickness of the current sheet. The solution is based on Harris-type shifted-Maxwellian particle distributions, with the ion velocity shift v_D in the y direction determined by $m_i v_T^2/LeB_0$ (where v_T is the ion thermal velocity).

[17] The two-dimensional solution reduces to the traditional 1-D *Harris* [1962] model if $F(x)$ equals 1. For a nonconstant $F(x)$, a finite B_z field appears, and its value at the center of the current sheet ($z = 0$) becomes

$$B_z(x,0) = -B_0 L F'(x)/F(x), \tag{5}$$

which in our present investigation is selected to have a constant value, B_n, with the assumption

$$F(x) = \exp[-(x/L)(B_n/B_0)]. \tag{6}$$

The self-consistent density distribution of the equilibrium is given by

$$n(x,z) = n_0 F^2(x)\,\mathrm{sech}^2[F(x)(z/L)], \tag{7}$$

which fulfills the initial condition with magnetic field and particle distribution function profiles self-consistently determined everywhere within the equilibrium current sheet. Figure 1 shows the magnetic field and density distributions of the initial equilibrium, with the following parameters: B_n = 1 nT, B_0 = 30 nT, n_0 = 0.7 cm^{-3}, v_T = 700 km/s, and L = 0.5 R_E. Next, the earthward propagating front, with magnetic and electric fields described by equations (1) and (2) is superimposed over the initial equilibrium, and test particle simulations are carried out to model the evolution of ion distributions during the approach of an earthward propagating dipolarization front.

[18] In our first run, we use the same dipolarization front parameters as those adopted by Zhou10: B_f = 10 nT, v_f = 250 km/s, L_f = 0.2 R_E. The virtual spacecraft is located within the tail current sheet (200 km north of the neutral sheet), and x_{f0}, the front initial location, is 5 R_E tailward of the spacecraft. The simulation, which stops at $t = t_0 + 127$ s (the front arrival time), results in the ion angular spectrum (in the energy range of 8–15 keV) of Figure 2a, which shows the appearance of the accelerated ion ahead of the front. Figure 2b shows the simulated evolution of the earthward flow velocity (the solid line) and the plasma density (the dashed line). Both of these values are shown to increase gradually, which is consistent with the gradual emergence of the accelerated, earthward streaming ion component. At the front arrival time, the earthward flow velocity is ~230 km/s, approximately equal to the front-propagating speed v_f, 250 km/s. These results are similar to those of Zhou10, however, in this simulation run, the accelerated ion population appears ~1 min before the front arrival, which agrees better with the observations and therefore resolves the aforementioned timing discrepancy.

[19] To elucidate the properties of the new ion population including its $\delta(t)$ value, we show the trajectory of a typical accelerated ion in Figure 3. The ion was selected from the energy and directions shown in Figure 2a, as denoted by the black dot. The ion is moving earthward and dawnward with kinetic energy of 15 keV when it reaches the spacecraft location 39 s ahead of the dipolarization front. Clearly the ion belongs to the superposed population, but is otherwise not special. Figure 3d shows that the kinetic energy of that ion increases by ~50% by $t \sim t_0 + 80$ s.

[20] The ion initially follows a cucumber-type trajectory within the equilibrium current sheet characterized by transitions between neutral sheet crossing and noncrossing elements [*Büchner and Zelenyi*, 1989]. In the xy plane (Figures 3a and 3b), this trajectory degenerates into a circular motion, with radius (~1.5 R_E) dictated by the ion gyroradius around the background B_z field of 1 nT. The kinetic energy of the ion stays constant until $t = t_0 + 75$ s when the ion encounters the approaching front and starts to gyrate around the enhanced B_z field. The gyrating motion lasts ~5 s, during which the kinetic energy of the ion increases by 5 keV due to the presence of the electric field (2) associated with the front. The ion is then reflected back to the region ahead of the front.

[21] This mechanism of ion reflection and concurrent acceleration is essentially the same as described by Zhou10. Contrary to the case of a zero background normal magnetic field (B_z = 0), however, in this case the ion does not stream unrestricted in the $+x$ direction. Instead, it starts to turn

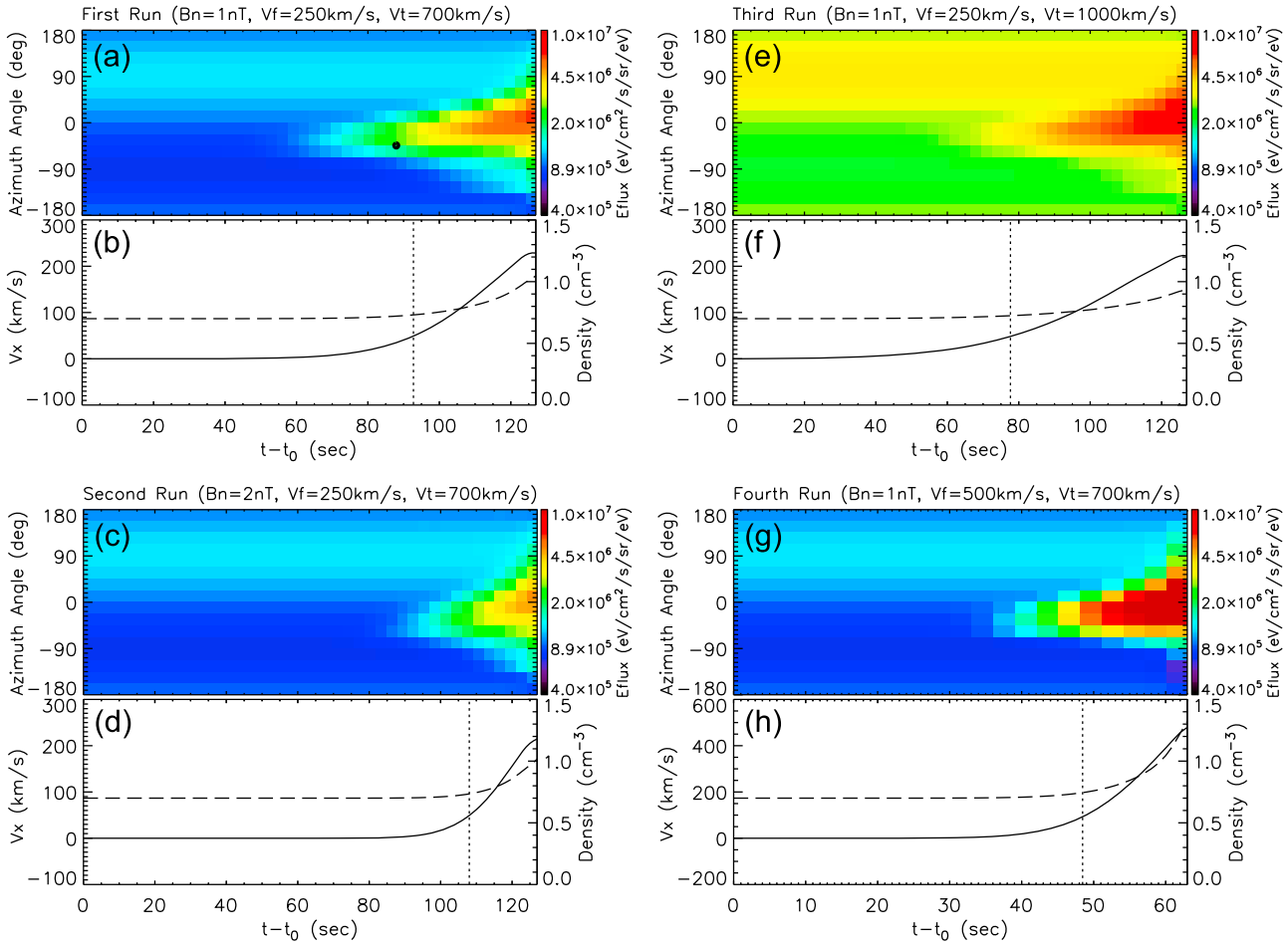

Figure 2. Results of our four simulation runs. Dipolarization front arrivals are at $t - t_0 = 127$ s for the first three runs and at $t - t_0 = 63$ s for the fourth run. (a, c, e, and g) Simulated ion differential energy flux versus equatorial azimuthal angle and time in the 8–15 keV energy range. Here 0° and 90° correspond to the earthward and duskward fluxes, respectively. (b, d, f, and h) Earthward plasma flow velocity and plasma density shown as solid and dashed lines, respectively. The vertical dotted lines correspond to the time when earthward flow velocity becomes significant (no less than 20% of the front propagation speed).

dawnward, executing a gyration around the finite background B_z of 1 nT. This is expected, since according to *Büchner and Zelenyi* [1989], ion motion within the current sheet is confined by its gyroradius around the background B_z. Consequently, the reflected ions, as well as the excursion of the related earthward flow and enhanced plasma density, would not be observed beyond the ion accessibility region, which is approximately one gyroradius earthward of the dipolarization front.

[22] Therefore, one would expect an inverse correlation between the magnitude of the background B_z field and the δt value. A second simulation run was constructed to test for this prediction, with a stronger B_z field, say, $B_n = 2$ nT, adopted in the initial equilibrium. All the other parameters remained the same as in the first run. The simulation results of the second run, displayed in Figures 2c and 2d, suggest features very similar to those produced in the first run (see Figures 2a and 2b), i.e., a gradual appearance of the superposed ion component over preexisting patterns, as well as increasing values of the plasma density and the earthward flow velocity (also converging toward v_f). The most significant difference between them, namely, the shorter duration of the accelerated ion population ahead of the dipolarization front, agrees well with the prediction.

[23] The size of the reflected ion accessibility region also depends on ion temperature. By increasing the ion thermal velocity v_T from 700 km/s to 1000 km/s in the third run, we examined the effect of a higher temperature on the resulting δt value. The simulation results are shown in Figures 2e and 2f. A similar evolution of the resultant ion distributions is clearly seen, although the ion fluxes of both preexisting and accelerated populations are much higher due to the higher initial temperature. If the appearance time of the earthward flow is defined as the time when v_x becomes greater than 20% of the front propagation speed v_f (which equals 50 km/s in this case), then $\delta t = 49$ s. In contrast, a value of 34 s is obtained in the first run with lower background temperature. This again agrees with the expectation that a higher ion temperature results in a larger ion accessibility region.

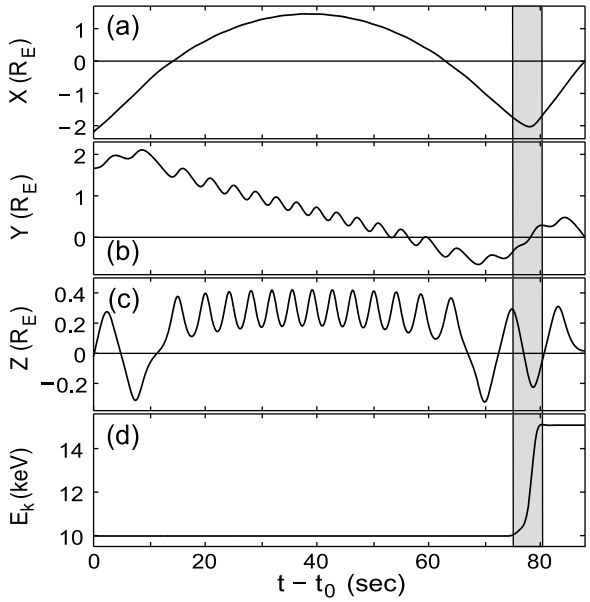

Figure 3. The trajectory of a typical ion obtained in the first simulation run: (a) x, (b) y, and (c) z locations and (d) the kinetic energy of the ion as functions of time. The time interval with the ion reflected and accelerated by the earthward propagating dipolarization front is represented by the shaded area.

[24] It should be further pointed out that δt is inversely correlated with the earthward propagating speed v_f of the dipolarization front, as a higher v_f value results in a shorter travel time of the dipolarization front across the entire region. The fourth simulation run tests this hypothesis, using the same parameters as in the first run except for a higher v_f value of 500 km/s. The simulation results are shown in Figures 2g and 2h. The δt value (15 s) is indeed approximately half the value in the first run (34 s). The higher propagation speed of the front is also consistent with a stronger ion acceleration thanks to the larger electric field of the front, and therefore is accompanied by higher fluxes of the reflected ion population over the same preexisting patterns.

[25] We conclude that the results of these simulation runs are consistent with the theoretical prediction: to first order, the time difference between the appearance of earthward flow and front arrival is proportional to the thermal ion gyroradius ahead of the front and inversely proportional to the earthward propagating speed of the dipolarization front. In other words,

$$\delta t \propto \frac{m v_T}{e B_n} \cdot \frac{1}{v_f}. \tag{8}$$

[26] It should be noted that the time difference does not depend on the value of B_f (the B_z enhancement associated with the front). By changing B_f in the first run from 10 nT to 5 nT, we obtained essentially the same results as Figure 2a (not shown). The result is not surprising, as the magnetic field behind the front cannot affect the ion trajectories ahead of it. In section 3, we examine the validity of equation (8) using statistical surveys of THEMIS observations.

3. Observations

[27] Before turning to the statistical surveys, we present an individual case study of the 26 February 2008 substorm/dipolarization front event [*Angelopoulos et al.*, 2008; *Pu et al.*, 2010] that indicates how the events were selected and how the relevant parameters in equation (8) were determined on the basis of observations.

[28] Figure 4 is a 3 min overview of the event observed by THEMIS P4, which was located in the near-Earth tail with GSM $x = -10.2\ R_E$. About 3 min after the initiation of magnetic reconnection at $x \sim 20\ R_E$ [*Angelopoulos et al.*, 2008], a strong B_z enhancement was observed by P4 at ~0453:25 UT indicating the arrival of a dipolarization front. Before front arrival, however, P4 had already observed gradual increases in earthward flow velocity and plasma density, as well as the appearance of an earthward streaming ion population superimposed over a preexisting steady duskward anisotropic ion population. All these features are expected signatures of reflected ions and resultant flows upstream of earthward propagating dipolarization fronts, in agreement with our simulations.

[29] We next examine observations from the THEMIS inner probes (P3, P4 and P5), taken during their first two tail seasons (from 1 February 2008 to 31 March 2008, and from

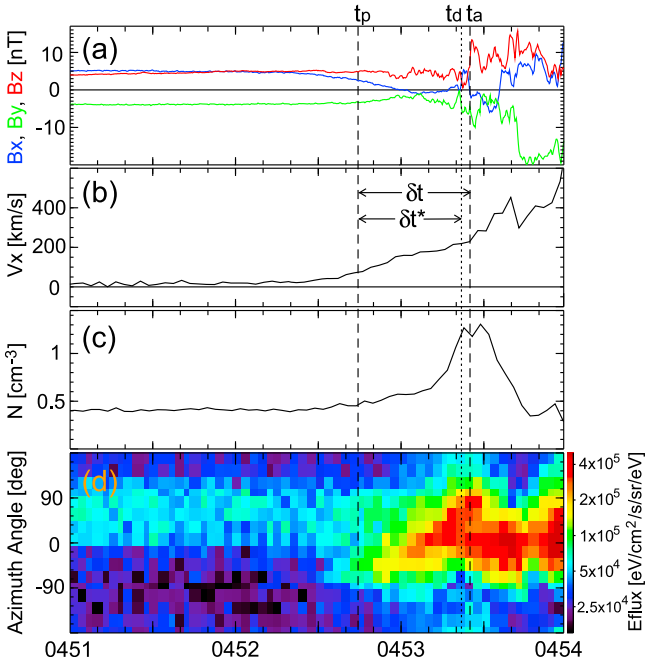

Figure 4. Overview of THEMIS P4 observations during the 26 February 2008 substorm or dipolarization front event. The two vertical dashed lines correspond to the dipolarization front arrival time t_a and the earthward flow onset time t_p, which define the precursor flow duration $\delta t = t_a - t_p$. (a) GSM magnetic field B_x, B_y, and B_z components. (b) Plasma flow velocity in the GSM x direction. (c) Plasma density. (d) Ion differential energy fluxes versus azimuth angle in the probe spin plane, as measured by the SST instrument in the 30–45 keV energy range.

1 February 2009 to 30 April 2009), and create a database of dipolarization front events. For each event, it is important that all of the relevant parameters (δt, v_f, B_n and v_T) could be unambiguously determined; this requires us to first specify operational definitions for these parameters. Using the 26 February 2008 event as a prototype (Figure 4), we introduce the steps we follow in the determination of these parameters for all events.

[30] 1. The front arrival time, t_a, is defined as the time with greatest enhancement in the low-pass-filtered (6 s running averaged) B_z within a 6 s interval. In the 26 February 2008 event, we have t_a = 0453:25 UT.

[31] 2. Contributions from both ESA [*McFadden et al.*, 2008] and SST [*Angelopoulos*, 2008] instruments are combined to accurately obtain the plasma data (including densities, flow velocities and thermal velocities). Contamination sources, such as sunlight and electronic contaminations in the energetic particle data from SST and the photoelectrons in the low-energy plasma data from ESA, are removed.

[32] 3. The earthward plasma velocity at t_a (245 km/s in our example) is assumed to be the earthward propagating speed v_f of the front. This definition is consistent with our simulation results showing that the earthward plasma velocity ahead of the front converges to v_f at $t = t_a$, and with recent observations [*Sergeev et al.*, 2009] showing the earthward propagating speed of the front (as determined by multispacecraft timing analysis) is the same as the measured plasma bulk velocity near the front.

[33] 4. We define the background velocity, v_b, as the average measured v_x velocity during the time interval between $t_a - 5$ min and $t_a - 2$ min.

[34] 5. We define the onset time of the earthward plasma flow, t_p, as the time when v_x reaches $v_b + (v_f - v_b)/5$. In our example, we have t_p = 0452:44 UT, shown in Figure 4, and $\delta t = t_a - t_p$ = 41 s.

[35] 6. We define the background thermal velocity, v_T, as the average measured ion thermal speed during the interval between $t_a - 5$ min and $t_a - 2$ min. In our example, this equals 841 km/s.

[36] 7. Finally, we define the normal magnetic field B_n of the equilibrium current sheet as the average B_z, from $t_a - 3$ min to $t_a - 10$ s; this is 4.5 nT in our case study.

[37] We select dipolarization front observed by the THEMIS inner probes in an automated fashion. To guarantee that the parameters δt, v_f, B_n and v_T are free of background noise, we use the following operational selection criteria.

[38] 1. The 6 s sliding average of B_z shows an enhancement greater than 5 nT per 6 s. Also the average B_z field, from t_a to t_a + 10 s, is at least 4 nT greater than the background B_n in the equilibrium current sheet.

[39] 2. The absolute value of the magnetic B_x component is smaller than 12 nT to ensure that the probe is inside the central part of the tail current sheet.

[40] 3. The earthward plasma velocity v_x at t_a is greater than 100 km/s, and the observed v_x value remains over 100 km/s for at least 40 s. This criterion is to ensure that the dipolarization front is embedded within earthward propagating bursty bulk flows. It eliminates the less frequent (albeit interesting) tailward or flankward events that could be due to recoil [e.g., *Panov et al.*, 2010], flow vortices [*Keiling et al.*, 2009] or slant crossings of the localized front surface.

[41] 4. The standard deviation of the v_x velocity observed between $t_a - 5$ min and $t_a - 2$ min is smaller than 15 km/s. Applied to guarantee that the v_b and δt values could be accurately determined, this criterion also ensures that the magnetotail current sheet is in equilibrium before front arrival.

[42] 5. The observed B_z, from $t_a - 3$ min to $t_a - 10$ s, has a standard deviation σ_{Bz} of no more than 1 nT. In addition, we required that B_n be at least twice as large as σ_{Bz} to ensure accurate determination of B_n and to guarantee an equilibrium state of the current sheet before front arrival.

[43] 6. The average B_y field, from $t_a - 3$ min to $t_a - 10$ s, has an absolute value of no more than 5 nT. This criterion eliminates events with strong guide field in the equilibrium current sheet, which is not considered in our simulation runs, and may significantly complicate the ion trajectory ahead of the front.

[44] The above criteria yielded a total of 36 dipolarization fronts, with an average δt value of 36 s. The parameters collected from each events were used to construct Figure 5a, where abscissa and ordinate of each black dot are the measured δt and mv_T/eB_nv_f values of each event.

[45] The linear regression fit to the data is shown as the solid line, and the correlation coefficient is 0.71. The prediction of equation (8) is thereby supported by the statistical survey of dipolarization fronts lending further credence to the suggestion that precursor flows in advance of dipolarization fronts are often composed of reflected ions confined within a thermal gyroradius around the normal field B_n ahead of the front.

[46] Despite the fair correlation between the left and right sides of equation (8) demonstrated in Figure 5a, it should also be pointed out that the slope of the fitted regression line (0.62) is smaller than that predicted from our simulations (see the dashed line in Figure 5a with the slope of 0.85). It is evident that the observed δt values are typically greater than the expected ones. The reason probably arises from the non-Maxwellian distributions of the ions in the equilibrium current sheet [e.g., *Christon et al.*, 1989; *Haaland et al.*, 2010], with energetic ions having greater fluxes than those expected from the assumed Maxwellian thermal speed. The presence of non-Maxwellian and/or superthermal ions is expected to result in a larger ion accessibility region earthward of the front than suggested by the simulation results.

[47] The fitted regression line also has an unexpected offset of 12.0 s in abscissa that does not appear in the simulations. One of the reasons may come from the transient B_z dip preceding the front. The very small B_z values within the dip, which usually last a few to few tens of seconds, would allow the reflected ions to keep moving in the earthward direction until they arrive at the region with unperturbed background B_z field and start their gyrations in the xy plane. This effect would enlarge the ion accessibility region and therefore enhance the δt values by a few to few tens of seconds.

[48] To evaluate this effect quantitatively, we subtracted the duration of each B_z dip from its corresponding δt value in all of the 36 events. The results, denoted as δt^*, are plotted versus mv_T/eB_nv_f in Figure 5b. This revised time delay δt^* between flow onset and B_z dip onset (also marked

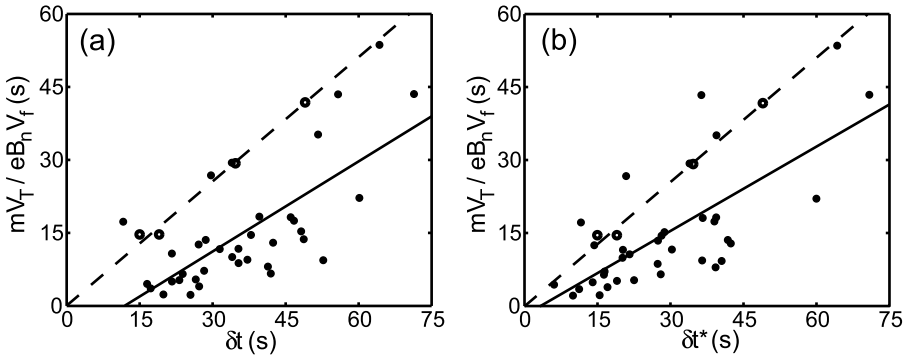

Figure 5. Scatterplots of 36 dipolarization front events found during the THEMIS 2008 and 2009 tail seasons. (a) The x and y locations of each solid point correspond to the left and right sides of equation (8), the δt and mv_T/eB_nv_f values of the corresponding event. The solid line is the fitted linear regression line of these data points, while the dashed line demarcates the expected linear relationship between these two values on the basis of our simulation results (denoted as the four black circles). (b) Same format as Figure 5a except that the δt values in abscissa are replaced by those values of δt* to eliminate the effects of the B_z dips that precede the fronts.

for our example case in Figure 4) is defined to end when the negative deviation of B_z from its equilibrium value, B_n, becomes significant (no less than 4 times over σ_{Bz} for at least 1 s). As evident in Figure 5b, the above correction results in a slightly higher correlation coefficient (0.71), and a significantly reduced abscissa offset (3.2 s).

[49] Another error source may arise from the three-dimensional nature of the dipolarization fronts [see *Runov et al.*, 2009, Figure 4b]. The front normal could significantly deviate from the x direction, and the probe crossings could be slanted. We plan to compile a larger database including more event studies and consider these complications to better understand the nature of earthward precursor flows in advance of the front.

4. Summary

[50] One of the most interesting observational features associated with the earthward propagating dipolarization fronts is the appearance of earthward plasma flows well before front arrival. These precursor flows are caused by the gradual emergence of a new ion population composed of ions that have been accelerated and reflected by the front (Zhou10).

[51] By incorporating a background northward magnetic field B_z in the equilibrium tail current sheet, we have further developed this model, and have shown that the reflected ions become confined to a region comparable to their thermal gyroradius over the background B_z upstream of the advancing front. Test particle simulations show a linear relationship between precursor flow duration δt and the typical gyroradius of the reflected ions. We have also carried out a statistical survey of THEMIS dipolarization fronts, which exhibit an average precursor flow commencement ~36 s prior to the front. The anticipated correlation between the thermal gyroradius of the reflected ion population and the precursor flow duration is shown to be consistent with the observations.

[52] The large variance in our data of Figure 5 suggests that other plasma acceleration mechanisms ahead of an approaching front cannot be excluded. In fact, the particle picture may be complementary to an MHD picture of the acceleration process such that the two processes may operate simultaneously. For example, a pressure gradient ahead of the front could be built up by the injection of the reflected ion population, which might result in acceleration of the ambient plasma [*Li et al.*, 2011] without direct interaction with the front itself. We also note that the front is localized in y, which means that the reflection process may be effective only on the earthward portion of the front where the front surface is expected to be sharpest and the ion acceleration strongest. Despite these caveats that require further studies, however, our simulations and the statistical significance of the front acceleration effect in the THEMIS data suggest that the mechanism of ion reflection and acceleration discussed herein is operational under many if not most conditions.

[53] **Acknowledgments.** We acknowledge NASA contract NAS5-02099 for making the THEMIS mission possible and supporting our work at UCLA. Our work at SPbU was also supported by RFBR grants 10-05-00223 and 10-05-91163. We thank K.-H. Glassmeier and U. Auster for the use of FGM data, J. P. McFadden for the use of ESA data, and D. Larson for the use of SST data. We are also grateful to P. Cruce, A. Flores, and J. Hohl for help with software and editing. One of the authors (X.-Z.Z.) would like to thank J. Liu and X. N. Chu for helpful discussions.

[54] Masaki Fujimoto thanks the reviewers for their assistance in evaluating this paper.

References

Angelopoulos, V. (2008), The THEMIS mission, *Space Sci. Rev.*, *141*, 5–34, doi:10.1007/s11214-008-9336-1.

Angelopoulos, V., W. Baumjohann, C. F. Kennel, F. V. Coroniti, M. G. Kivelson, R. Pellat, R. J. Walker, H. Lühr, and G. Paschmann (1992), Bursty bulk flows in the inner central plasma sheet, *J. Geophys. Res.*, *97*, 4027–4039.

Angelopoulos, V., C. Kennel, F. Coroniti, R. Pellat, M. Kivelson, R. Walker, C. Russell, W. Baumjohann, W. Feldman, and J. Gosling (1994), Statistical characteristics of bursty bulk flow events, *J. Geophys. Res.*, *99*, 21,257–21,280, doi:10.1029/94JA01263.

Angelopoulos, V., et al. (2008), Tail reconnection triggering substorm onset, *Science*, *321*, 931–935, doi:10.1126/science.1160495.

Büchner, J., and L. M. Zelenyi (1989), Regular and chaotic charged particle motion in magnetotaillike field reversals: 1. Basic theory of trapped motion, *J. Geophys. Res.*, *94*, 11,821–11,842.

Chen, C. X., and R. A. Wolf (1993), Interpretation of high-speed flows in the plasma sheet, *J. Geophys. Res.*, *98*, 21,409–21,419, doi:10.1029/93JA02080.

Christon, S. P., D. J. Williams, D. G. Mitchell, L. A. Frank, and C. Y. Huang (1989), Spectral characteristics of plasma sheet ion and electron populations during undisturbed geomagnetic conditions, *J. Geophys. Res.*, *94*, 13,409–13,424, doi:10.1029/JA094iA10p13409.

Dubyagin, S., V. A. Sergeev, S. Apatenkov, V. Angelopoulos, R. Nakamura, J. McFadden, D. Larson, and J. Bonnell (2010), Pressure and entropy changes in the flow-braking region during magnetic field dipolarization, *J. Geophys. Res.*, *115*, A10225, doi:10.1029/2010JA015625.

Haaland, S., E. A. Kronberg, P. W. Daly, M. Fränz, L. Degener, E. Georgescu, and I. Dandouras (2010), Spectral characteristics of protons in the Earth's plasmasheet: Statistical results from Cluster CIS and RAPID, *Ann. Geophys.*, *28*, 1483–1498.

Harris, E. G. (1962), On a plasma sheath separating regions of oppositely directed magnetic field, *Nuovo Cimento*, *23*, 115–121.

Keiling, A., et al. (2009), Substorm current wedge driven by plasma flow vortices: THEMIS observations, *J. Geophys. Res.*, *114*, A00C22, doi:10.1029/2009JA014114.

Lembége, B., and R. Pellat (1982), Stability of a thick two-dimensional quasineutral sheet, *Phys. Fluids*, *25*, 1995–2004.

Li, S.-S., V. Angelopoulos, A. Runov, X.-Z. Zhou, J. P. McFadden, D. Larson, J. Bonnell, and U. Auster (2011), On the force balance around dipolarization fronts within bursty bulk flows, *J. Geophys. Res.*, doi:10.1029/2010JA015884, in press.

Lui, A. T. Y., R. E. Lopez, S. M. Krimigis, R. W. McEntire, L. J. Zanetti, and T. A. Potemra (1988), A case study of magnetotail current sheet disruption and diversion, *Geophys. Res. Lett.*, *15*, 721–724.

Manankova, A. V. (2003), Two-dimensional current-carrying plasma sheet in the near-Earth geomagnetic tail region: A quasi-stationary evolution, *Ann. Geophys.*, *21*, 2259–2269.

McFadden, J. P., C. W. Carlson, D. Larson, M. Ludlam, R. Abiad, B. Elliott, P. Turin, M. Marckwordt, and V. Angelopoulos (2008), The THEMIS ESA plasma instrument and in-flight calibration, *Space Sci. Rev.*, *141*, 277–302, doi:10.1007/s11214-008-9440-2.

McPherron, R. L., C. T. Russell, and M. P. Aubrey (1973), Satellite studies of magnetospheric substorms on August 15, 1968: 9. Phenomenological model for substorms, *J. Geophys. Res.*, *78*, 3131–3149.

Nakamura, R., et al. (2002), Motion of the dipolarization front during a flow burst event observed by Cluster, *Geophys. Res. Lett.*, *29*(20), 1942, doi:10.1029/2002GL015763.

Ohtani, S., M. A. Shay, and T. Mukai (2004), Temporal structure of the fast convective flow in the plasma sheet: Comparison between observations and two-fluid simulations, *J. Geophys. Res.*, *109*, A03210, doi:10.1029/2003JA010002.

Panov, E. V., et al. (2010), Multiple overshoot and rebound of a bursty bulk flow, *Geophys. Res. Lett.*, *37*, L08103, doi:10.1029/2009GL041971.

Pontius, D. H., Jr., and R. A. Wolf (1990), Transient flux tubes in the terrestrial magnetosphere, *Geophys. Res. Lett.*, *17*, 49–52, doi:10.1029/GL017i001p00049.

Pritchett, P. L., and J. Büchner (1995), Collisionless reconnection in configurations with a minimum in the equatorial magnetic field and with magnetic shear, *J. Geophys. Res.*, *100*, 3601–3611, doi:10.1029/94JA03028.

Pu, Z. Y., et al. (2010), THEMIS observations of substorms on 26 February 2008 initiated by magnetotail reconnection, *J. Geophys. Res.*, *115*, A02212, doi:10.1029/2009JA014217.

Runov, A., V. Angelopoulos, M. I. Sitnov, V. A. Sergeev, J. Bonnell, J. P. McFadden, D. Larson, K. Glassmeier, and U. Auster (2009), THEMIS observations of an earthward-propagating dipolarization front, *Geophys. Res. Lett.*, *36*, L14106, doi:10.1029/2009GL038980.

Runov, A., et al. (2011a), Dipolarization fronts in the magnetotail plasma sheet, *Planet. Space Sci.*, doi:10.1016/j.pss.2010.06.006, in press.

Runov, A., V. Angelopoulos, X.-Z. Zhou, X.-J. Zhang, S. Li, F. Plaschke, and J. Bonnell (2011b), A THEMIS multi-case study of dipolarization fronts in the magnetotail plasma sheet, *J. Geophys. Res.*, doi:10.1029/2010JA016316, in press.

Schindler, K. (1972), A self-consistent theory of the tail of the magnetosphere, in *Earth's Magnetospheric Processes*, *Astrophys. Space Sci. Libr.*, vol. 32, edited by B. M. McCormac, p. 200, D. Reidel, Dordrecht, Netherlands.

Schindler, K., and J. Birn (2002), Models of two-dimensional embedded thin current sheets from Vlasov theory, *J. Geophys. Res.*, *107*(A8), 1193, doi:10.1029/2001JA000304.

Schwartz, S. J., P. W. Daly, and A. N. Fazakerley (1998), Multi-spacecraft analysis of plasma kinetics, in *Analysis Methods for Multi Spacecraft Data*, edited by G. Paschmann and P. W. Daly, pp. 159–184, Eur. Space Agency, Bern.

Semenov, V. S., T. Penz, V. V. Ivanova, V. A. Sergeev, H. K. Biernat, R. Nakamura, M. F. Heyn, I. V. Kubyshkin, and I. B. Ivanov (2005), Reconstruction of the reconnection rate from Cluster measurements: First results, *J. Geophys. Res.*, *110*, A11217, doi:10.1029/2005JA011181.

Sergeev, V. A., R. C. Elphic, F. S. Mozer, A. Saint-Marc, and J. A. Sauvaud (1992), A two satellite study of nightside flux transfer events in the plasma sheet, *Planet. Space Sci.*, *40*, 1551–1572, doi:10.1016/0032-0633(92)90052-P.

Sergeev, V. A., T. I. Pulkkinen, and R. I. Pellinen (1996), Coupled-mode scenario for the magnetospheric dynamics, *J. Geophys. Res.*, *101*, 13,047–13,065.

Sergeev, V. A., V. Angelopoulos, S. Apatenkov, J. Bonnell, R. Ergun, R. Nakamura, J. P. McFadden, D. Larson, and A. Runov (2009), Kinetic structure of the sharp injection/dipolarization front in the flow-braking region, *Geophys. Res. Lett.*, *36*, L21105, doi:10.1029/2009GL040658.

Sergeev, V. A., V. Angelopoulos, M. V. Kubyshkina, E. Donovan, X.-Z. Zhou, A. Runov, H. Singer, J. P. McFadden, and R. Nakamura (2011), Substorm growth and expansion onset as observed with ideal ground-spacecraft THEMIS coverage, *J. Geophys. Res.*, *116*, A00I26, doi:10.1029/2010JA015689.

Sibeck, D. G., and V. Angelopoulos (2008), THEMIS science objectives and mission phases, *Space Sci. Rev.*, *141*, 35–59, doi:10.1007/s11214-008-9393-5.

Sitnov, M. I., M. Swisdak, P. N. Guzdar, and A. Runov (2006), Structure and dynamics of a new class of thin current sheets, *J. Geophys. Res.*, *111*, A08204, doi:10.1029/2005JA011517.

Sitnov, M. I., M. Swisdak, and A. V. Divin (2009), Dipolarization fronts as a signature of transient reconnection in the magnetotail, *J. Geophys. Res.*, *114*, A04202, doi:10.1029/2008JA013980.

Slavin, J. A., R. P. Lepping, J. Gjerloev, D. H. Fairfield, M. Hesse, C. J. Owen, M. B. Moldwin, T. Nagai, A. Ieda, and T. Mukai (2003), Geotail observations of magnetic flux ropes in the plasma sheet, *J. Geophys. Res.*, *108*(A1), 1015, doi:10.1029/2002JA009557.

Wanliss, J. A., R. D. Sydora, G. Rostoker, and R. Rankin (2002), Origin of some anisotropic tailward flows in the plasma sheet, *Ann. Geophys.*, *20*, 1559–1575.

Yoon, P. H., and A. T. Y. Lui (2004), Model of ion- or electron-dominated current sheet, *J. Geophys. Res.*, *109*, A11213, doi:10.1029/2004JA010555.

Zhang, X.-J., V. Angelopoulos, A. Runov, X.-Z. Zhou, J. Bonnell, J. P. McFadden, D. Larson, and U. Auster (2011), Current-carriers near dipolarization fronts in the magnetotail: A THEMIS event study, *J. Geophys. Res.*, *116*, A00I20, doi:10.1029/2010JA015885.

Zhou, X.-Z., V. Angelopoulos, A. Runov, M. I. Sitnov, Q.-G. Zong, and Z. Y. Pu (2009a), Ion distributions near the reconnection sites: Comparison between simulations and THEMIS observations, *J. Geophys. Res.*, *114*, A12211, doi:10.1029/2009JA014614.

Zhou, X.-Z., et al. (2009b), Thin current sheet in the substorm late growth phase: Modeling of THEMIS observations, *J. Geophys. Res.*, *114*, A03223, doi:10.1029/2008JA013777.

Zhou, X.-Z., V. Angelopoulos, V. A. Sergeev, and A. Runov (2010), Accelerated ions ahead of earthward propagating dipolarization fronts, *J. Geophys. Res.*, *115*, A00I03, doi:10.1029/2010JA015481.

Zong, Q.-G., et al. (2004), Cluster observations of earthward flowing plasmoid in the tail, *Geophys. Res. Lett.*, *31*, L18803, doi:10.1029/2004GL020692.

V. Angelopoulos, A. Runov, and X.-Z. Zhou, Institute of Geophysics and Planetary Physics, University of California, Los Angeles, CA 90065-1567, USA. (xzhou@igpp.ucla.edu)

V. A. Sergeev, Institute of Physics, St. Petersburg State University, St. Petersburg 198904, Russia.